STABILIZATION OF LIPOSOMAL FUNCTIONAL ANCHORS BY CROSS-LINKABLE LIPIDS

BY

CARTNEY EATON SMITH

THESIS

Submitted in partial fulfillment of the requirements
for the degree of Master of Science in Chemical Engineering
in the Graduate College of the
University of Illinois at Urbana-Champaign, 2013

Urbana, Illinois

Adviser:

Assistant Professor Hyunjoon Kong

ABSTRACT

Micro- and nanoparticles are designed to deliver drugs and contrast agents to their target site in a controlled manner. One of the greatest obstacles in the performance of such delivery vehicles is their stability in the presence of serum. Here we investigate a method to stabilize a class of liposomes in which lipid vesicles are modified post-fabrication through surface adsorption and anchoring. We hypothesized that the sequential adsorption of functional units followed by covalent cross-linking of the liposome would provide enhanced stability in the presence of human serum. To investigate this hypothesis, liposomes composed of diyne-containing lipids were assembled and functionalized via chitosan conjugated with a hydrophobic anchor and the magnetic resonance (MR) contrast agent, gadolinium, as a model functionality. This strategy served to stabilize the thermodynamically favorable association between liposome and modified functional chitosan. Furthermore, the chitosan-coated, cross-linked liposomes proved more effective as delivery vehicles of MR contrast agents than uncross-linked liposomes due to the reduced liposome degradation and chitosan desorption. Overall, this study demonstrates a useful method to stabilize a broad class of particles used for systemic delivery of various molecular cargos.

TABLE OF CONTENTS

CHAPTER 1: INTRODUCTION 1

CHAPTER 2: MATERIALS AND METHODS 4

CHAPTER 3: RESULTS AND DISCUSSION 9

CHAPTER 4: CONCLUSION 25

REFERENCES 28

Chapter 1

INTRODUCTION

1.1 Background and Motivation

The use of micro- and nanoparticles has dramatically improved the efficacy of diagnostic and therapeutic agents for various biomedical applications. Encapsulation of hydrophobic drugs, for example, allows for the delivery of pharmaceuticals that would otherwise be insoluble.[1] Furthermore, by altering the size, shape, and surface charge, the biodistribution and cellular uptake pathways of the nanoparticle can be tailored for its particular application.[2-4] In addition, the particle may be conjugated with ligands to enhance retention[5] or deliver the encapsulated agent to a target site of interest.[6, 7] Taken together, these attributes have allowed for lower drug dosing, reduced toxicity, and enhanced efficacy of therapies, as well as the capability of sensitive diagnostics to probe *in vivo* microenvironments.

One of the main challenges in translating nanoparticle formulations from benchtop to clinic is *in vivo* stability. While biomedical nanomaterials may demonstrate the desired functionality in a controlled setting, the expected performance may not be realized in the dynamic environment of the circulatory system due to premature degradation and disassembly of the nanoparticle. One reason for such incidence is related to the thermodynamic stability of the particle upon dilution. Below the critical micelle concentration (CMC) of a self-assembled structure, the material will dissociate, in which case delivery becomes an issue of kinetics of disassembly versus transport to the target site.[8] Secondly, another factor that determines stability in the presence of serum is protein

adsorption. The non-specific binding of serum proteins to the nanoparticle surface causes opsonization, and affects biodistribution and cellular uptake.[9, 10] Though this can be reduced with attachment of poly(ethylene glycol) (PEG) to the surface, there is still a need to develop more effective methods to minimize serum-inducing destabilization. Thirdly, serum presents a harsh environment due to degradative enzymes that can actively digest certain biomaterials that make up nanoparticle formulations, as well as charged proteins that can disrupt electrostatic interactions. The kinetics of such processes are often activated or enhanced at the elevated temperature of 37 °C. For these reasons, it is important to improve nanoparticle stability under physiologically relevant conditions.[11]

We recently developed a strategy of modular surface assembly in which a functional unit could be non-covalently attached to a liposome surface post-fabrication through electrostatic and hydrophobic interactions between the liposome and a chitosan anchor. Due to the factors described above, liposomes are inherently unstable *in vivo* and, depending on composition, can be cleared within hours.[12] Therefore, to stabilize the chitosan anchor, it is strategic to not only stabilize its association with lipids, but to also stabilize the liposome itself. Additionally, it is beneficial to cross-link the liposome rather than to perform chemical conjugation to the particle surface due to the inefficiency of surface reactions and subsequent purification steps needed, which can be costly and damaging to the liposome.[13]

1.2 Research Plan

In this study we examined liposomes composed of cross-linkable lipids and their effect on the stability of the chitosan anchor in the presence of serum-supplemented

media. The sequential anchoring of the modified chitosan followed by cross-linking of diyne lipids via UV irradiation was found to be critical in achieving stability enhancement, as supported by thermodynamic analysis. The importance of such stabilization was demonstrated through the use of the model chitosan anchor in this study, which contained the gadolinium chelate, diethylenetriaminepentaacetic acid (DTPA). The sequential adsorption and cross-linking steps provided enhanced magnetic resonance (MR) signal contrast after one hour in serum-supplemented media compared to liposomes that were cross-linked prior to chitosan adsorption. The results of this study will be of great benefit in stabilizing liposomes modified with a wide variety of functional moieties through modular surface assembly.

Chapter 2

MATERIALS AND METHODS

2.1 Synthesis and Characterization of DTPA-Chitosan-g-C_{18}

Briefly, chitosan (Sigma-Aldrich) was dissolved at pH 4.7 and reacted with stearic acid (Sigma-Aldrich) to create the hydrophobic anchor. The amide formation was mediated by 1-ethyl-3-(3-dimethylaminopropyl) carbodiimide (EDC, Sigma-Aldrich). The resultant chitosan-g-C_{18} was then precipitated in sodium hydroxide and re-dissolved with hydrochloric acid twice. Afterwards, DTPA (Sigma-Aldrich) was dissolved with Tetramethylethylenediamine (TEMED, Sigma-Aldrich) and reacted with chitosan-g-C_{18} by EDC-mediated amide formation once again. The product was purified by dialysis (MWCO 6,000-8,000, Fisher Scientific), lyophilized, and stored as a powder.

The degree of substitution of the alkyl chain was quantified by 2,4,6-trinitrobenzene sulfonic acid (TNBS, Sigma-Aldrich), which was used as a colorimetric assay for primary amines to determine the number of remaining, unconjugated glucosamine units. The degree of substitution of DTPA was measured by titration of DTPA-chitosan-g-C_{18} with gadolinium ($GdCl_3 \bullet 6H_2O$, Sigma-Aldrich) in the presence of xylenol orange (Sigma-Aldrich). With each addition of gadolinium, an aliquot was mixed with xylenol orange until the color changed from yellow to pick, indicating saturation of DTPA and thus the molar amount of DTPA could be calculated.

2.2 Liposome Fabrication

1,2-bis(10,12-tricosadiynoyl)-*sn*-glycero-3-phosphocholine ($DC_{8,9}PC$, Avanti Polar Lipids) was dissolved in chloroform at a concentration of 20 mg/mL. During all handling of lipids, samples were protected from light to avoid unintended cross-linking. The lipid solution was transferred to a 50 mL capacity round bottom flask and the chloroform was removed by rotary evaporation, leaving a thin lipid film. The film was then hydrated with deionized water at 50 °C to a lipid concentration of 1 mg/mL. Liposomes were then cooled in an ice bath, sonicated for 15 minutes, and stored at 4 °C.

2.3 Liposome Coating and Cross-Linking

To coat pre-formed vesicles, liposomes were incubated with a DTPA-chitosan-g-C_{18} solution at a molar ratio of 5:1 glucosamine unit to outer leaflet lipid. To ensure equilibration, the mixture stirred overnight. Excess chitosan was then removed by centrifugation for 10 minutes at 4,000 rpm to pellet the liposomes. Non-adsorbed chitosan remaining in the supernatant was removed and the coated liposomes were re-suspended in deionized water.

Cross-linking of lipids was carried out either before or after binding with modified chitosan. In either case, lipids were cross-linked for 10 minutes at 4 °C with light at a wavelength of 254 nm (Jelight Co.). After cross-linking, the liposome suspension appeared orange in color.

2.4 Binding and Stability of Fluorescently Labeled DTPA-Chitosan-g-C_{18}

To quantify the amount of chitosan associated with liposomes, DTPA-chitosan-g-C_{18} was first fluorescently labeled. Briefly, the modified chitosan was dissolved in deionized water and incubated overnight with a solution of the amine reactive fluorophore, rhodamine B isothiocyanate (Sigma-Aldrich). Following conjugation, excess rhodamine was removed by dialysis and the labeled chitosan was lyophilized. For quantitation, fluorescent DTPA-chitosan-g-C_{18} was dissolved in deionized water and incubated with liposomes as described. Then, following purification by centrifugation, the fluorescent intensities of the supernatant and re-suspended liposomes were analyzed by microplate reader (Tecan Infinite 200 PRO, Tecan AG, Switzerland) with excitation at 535 nm and emission at 595 nm.

To examine the stability of the association under stressed conditions, coated liposomes were re-suspended in serum-supplemented media rather than deionized water after removal of excess fluorescent chitosan. Media consisted of 10% type AB human serum off the clot (PAA Laboratories Inc.) in phosphate buffered saline (PBS). Samples re-suspended in the serum media were then incubated at 37 °C. At each time point, 30 and 60 minutes, a sample was removed from incubation and centrifuged for 10 minutes at 4,000 rpm. It was then re-suspended and analyzed for fluorescent intensity to determine how much of the initial amount had been desorbed into the supernatant. Background interference from serum, though minimal, was subtracted from the experimental samples for accurate quantitation.

2.5 Thermodynamics of Binding Between DTPA-Chitosan-g-C_{18} and Cross-Linkable Liposomes

Isothermal titration calorimetry (ITC) was carried out with a VP-ITC calorimeter (MicroCal, Northampton, MA). Experiments were performed at 25 °C with DTPA-chitosan-g-C_{18} at a concentration of 5 mM glucosamine unit titrated into the 1.45 mL well of liposome suspension. 28 injections were made over 17.1 s each with a delay of 300 s between injections. The injection volume was 10 μL and the syringe stirred at 310 rpm. Analysis was done with Origin 5.0 software from MicroCal using a single-site binding model.

2.6 Magnetic Resonance Imaging of Gadolinium-Loaded Liposomes

To prepare gadolinium-loaded liposomes, the lipid vesicles were incubated with DTPA-chitosan-g-C_{18} as described. Then, after removal of free chitosan by centrifugation, gadolinium was added incrementally until all DTPA binding sites on the liposome surface were occupied, as indicated by xylenol orange assay. Samples were then incubated at 37 °C with 10% serum in PBS. After one hour, samples were centrifuged again to remove gadolinium-bound DTPA-chitosan-g-C_{18} that was desorbed during incubation. To prepare the samples for MRI, a concentration series was made using borosilicate cell culture tubes. The tubes were then placed in an agar gel to immobilize the samples and reduce imaging artifacts.

Imaging was completed with a 3 T Siemens Magnetom Trio clinical scanner (Siemens AG, Erlangen, Germany). Image acquisition was performed with an inversion recovery turbo spin echo (IR-TSE) sequence with a slice thickness of 3.0 mm, repetition

time (*TR*) of 2,500 ms, echo time (*TE*) of 18.0 ms, and inversion time (*TI*) ranging from 100 to 1,700 ms. For each *TI*, signal intensity was measured using ImageJ software and used to determine the spin-lattice relaxation time (T_1) of each phantom by non-linear least squares curve fitting.

To determine molar relaxivity, the concentration of gadolinium per sample was ascertained by inductively couple plasma optical emission spectroscopy (ICP-OES, Perkin Elmer Optima 2000 DV, Norwalk, CT). Prior to analysis, samples were digested in nitric acid to induce sample degradation. Relaxation rate was plotted against gadolinium concentration and relaxivity was determined by linear regression.

Chapter 3

RESULTS AND DISCUSSION

3.1 Formulation of Liposomes Coated with DTPA-Chitosan-g-C_{18}

Liposomes were formed by film hydration of 1,2-bis(10,12-tricosadiynoyl)-*sn*-glycero-3-phosphocholine, termed $DC_{8,9}PC$, lipids. As shown in Figure 1a, $DC_{8,9}PC$ lipids are cross-linked upon UV irradiation at 254 nm. This is due to the diyne functionality, in which alkynes on adjacent hydrophobic chains are able to bond and polymerize the liposome. This strategy has been used to create local regions of reduced mobility within mixed lipid bilayers for photo-triggered drug release.[14] However, in the case of liposomes formed solely with $DC_{8,9}PC$, cross-linking induces a continuous shell within the bilayer. Successful cross-linking was indicated by a color change of the liposome suspension from white to orange (Figure 1b).

In previous work, we developed a chitosan modified with the gadolinium chelate, DTPA, and an 18-carbon hydrophobic anchor (unpublished data). Chitosan, a polysaccharide consisting of glucosamine repeat units, has previously been shown to adsorb to liposome surfaces primarily through electrostatic associations, and to a lesser extent, hydrophobic interactions, hydrogen bonding, and van der Waals forces.[15] In our case, the DTPA-modified glucosamine unit served not only to chelate gadolinium for MRI contrast enhancement, but also provided additional electrostatic interaction and afforded water solubility at neutral or physiological pH to the chitosan backbone. The 18-carbon anchor takes advantage of the fluid-like nature of the liposome structure by inserting into the hydrophobic region of the bilayer. The degree of substitution of DTPA

(DS_{DTPA}) was found to be 15.4%, while that of the alkyl chain (DS_{C18}) was 4.2%. In the present study, to create the liposome-chitosan association, the functionalized chitosan was dissolved in deionized water and mixed with pre-formed lipid vesicles. In the case of $DC_{8,9}PC$-based liposomes, chitosan was incubated at a 5:1 glucosamine unit-to-outer leaflet lipid ratio to induce adsorption and saturate the liposome surface.

Here, we examined three liposome-chitosan systems (Figure 2). In the first case, the functionalized chitosan was adsorbed to $DC_{8,9}PC$ liposomes without inducing the cross-linking reaction. The second case consisted of adsorbing chitosan to pre-cross-linked liposomes. Thirdly, we investigated the system in which chitosan was first adsorbed to the liposome, followed by cross-linking of lipids afterwards.

3.2 Evaluation of DTPA-Chitosan-g-C_{18} Binding to Cross-Linkable Liposomes

To quantify the binding stoichiometry between modified chitosan and liposome in each of the three cases, DTPA-chitosan-g-C_{18} was fluorescently labeled with rhodamine-B isothiocyanate, which readily reacted with the primary amine groups on unmodified glucosamine units. In this way, it was possible to analyze the fluorescent intensity of re-suspended liposomes, as well as supernatant, after centrifugation to remove free chitosan and pellet the vesicles. Fluorescent intensity was used for quantitation by relating it to calibration against known chitosan concentration. Binding stoichiometry was defined in terms of the ratio between glucosamine repeat unit to exposed lipid on the outer leaflet, which is assumed to be half of the total lipids. Results for the three cases tested after incubation with a five-fold molar excess of glucosamine units are shown in Figure 3.

In the two cases where the modified chitosan was initially adsorbed to uncross-linked liposomes, the binding stoichiometry was nearly 2.5:1 glucosamine unit-to-exposed lipid. The polymerization of the lipids did not induce desorption, nor provide a mechanism of additional adsorption of chitosan, since the binding stoichiometry was equivalent between liposomes cross-linked after adsorption to liposomes that were not cross-linked at all. Interestingly, however, in the case where DTPA-chitosan-g-C_{18} was incubated with pre-cross-linked liposomes, the binding was 1:1. In this way, polymerization of the bilayer interfered with the ability of the liposome to bind with chitosan. This may be due to steric hindrance as lipids adopt a rigid conformation that may be unfavorable for interaction with the chitosan. Similarly, by reducing the fluidity of the bilayer, lipids cannot rotate or translocate to accommodate the binding. In particular, the hydrophobic anchor may not be able to insert into the rigid bilayer.

To further examine the binding between liposome and chitosan, isothermal titration calorimetry (ITC) was performed. Liposomes were formed by film hydration as described, and then titrated with DTPA-chitosan-g-C_{18}. The case of uncross-linked liposomes was compared to those that were cross-linked to determine whether cross-linked lipids would be detrimental to the thermodynamic association between liposome and chitosan. The resultant thermograms are shown in Figure 4.

From the heat flow data, it is apparent that in both cases, the association was endothermic as indicated by the positive change in heat with each injection of DTPA-chitosan-g-C_{18}. As shown previously, the interaction between chitosan and similar zwitterionic lipids can present an increase in enthalpy.[16] To extract binding ratios, binding constant, and enthalpy of association from the raw data in Figure 4, a single-site

binding model was applied.[17] This model can be derived by first defining the binding constant as follows:

$$K = \frac{X}{(1-X)C_{free}} \tag{1}$$

where X is the fraction of lipids bound by DTPA-chitosan-g-C_{18}, and C_{free} is the concentration of glucosamine unit that remains free in solution rather than bound to a liposome. This can be related to the total glucosamine concentration, C_t as shown in Equation 2:

$$C_t = C_{free} + NXL_t \tag{2}$$

in which the quantity NXL_t represents the concentration of bound glucosamine with N representing the binding ratio and L_t as the total lipid concentration. Combining Equations 1 and 2 yields the following quadratic equation:

$$X^2 - X\left(1 + \frac{C_t}{NL_t} + \frac{1}{NKL_t}\right) + \frac{C_t}{NL_t} = 0 \tag{3}$$

With the parameters C_t and L_t known by experimental design, it is necessary to relate X to the measured heat flow data to determine N and K, as well as enthalpy, ΔH. This is done by relating the heat content of solution, Q, in its volume, V_0, and substituting into Equation 3:

$$Q = NXL_t\Delta HV_0 \tag{4}$$

$$Q = \frac{NL_t\Delta HV_0}{2}\left[1 + \frac{C_t}{NL_t} + \frac{1}{NKL_t} - \sqrt{\left(1 + \frac{C_t}{NL_t} + \frac{1}{NKL_t}\right)^2 - \frac{4C_t}{NL_t}}\right] \tag{5}$$

By fitting heat flow data for each successive injection, it is then possible to extract the fit parameters of N, K, and ΔH. For the two systems examined, these data are summarized in Table 1.

As in the study described in the previous section, the binding ratio (N) between the glucosamine units and total lipids was more than two-fold greater in the case of uncross-linked liposomes compared to those that were pre-cross-linked. Additionally, the binding constant, K, was also greater in the case of uncross-linked liposomes. This can be translated to the change in Gibb's free energy as follows:

$$\Delta G = -RT\ln(K) \tag{6}$$

where T is temperature and R is the universal gas constant. Accordingly, ΔG was more negative, hence more thermodynamically favorable, in the case of lipids that were not cross-linked. It has been demonstrated previously that insertion of a hydrophobic domain into a lipid bilayer contributes to the negative change in ΔG.[18, 19] Therefore the differences in ΔG are consistent with the hypothesis that in the case of pre-cross-linked liposomes, the 18-carbon anchor attached to chitosan has a more limited capability to insert into the liposome and provide anchoring. This is depicted schematically in Figure 2 as the case where the alkyl chain either does not insert, thus remaining in the aqueous exterior, or inserts only partially into the bilayer. In either case, the binding would not be as favorable, and the association weaker.

This is also in agreement with the trend in change in entropy, ΔS, which is determined from the other thermodynamic parameters as follows:

$$\Delta S = \frac{\Delta H - \Delta G}{T} \tag{7}$$

The entropy-driven process was previously shown to be enhanced by the entropic contribution of the alkyl chain insertion (unpublished data). This is due to the desolvation of water molecules surrounding the 18-carbon chain, and the gain in configurational entropy they acquire in doing so, consistent with the hydrophobic effect.[20, 21] Therefore, the smaller change in entropy in the case of the cross-linked liposome may again be due to incomplete insertion of the alkyl anchor as a result of the cross-linking.

3.3 Stability of Liposome Coatings in Serum

As serum can be detrimental to the stability of assembled structures *in vivo*, it is important to assess stability in its presence. Here, we monitored the stability of the chitosan-liposome association in 10% human serum in PBS at 37 °C. Rhodamine-labeled DTPA-chitosan-g-C_{18} was incubated overnight with $DC_{8,9}PC$ liposomes in the three cases described: no cross-linking, pre-adsorption cross-linking, and post-adsorption cross-linking. Excess chitosan was then removed by centrifugation, and the coated liposomes were re-suspended in the serum solution. At 30 and 60 minutes, samples were pelleted and re-suspended again to determine how much of the fluorescent chitosan remained with the liposomes versus desorption and collection into supernatant. The results are shown in Figure 5.

The percent of coated liposomes remaining was determined from the amount of coated liposomes at the time points tested compared to liposomes prior to serum addition. In the cases of uncross-linked liposomes and liposomes cross-linked prior to addition of the modified chitosan, more than half of the chitosan was desorbed over the course of an hour in serum. There was no statistical difference in the percent desorbed between these

two cases. However, when DTPA-chitosan-g-C_{18} was adsorbed to the liposome prior to cross-linking, the enhancement was dramatic. Approximately 75% of the initial amount adsorbed remained after 30 minutes, and no further desorption was observed for the remainder of the hour in serum. The mechanism of stabilization is likely two-fold: stabilization of the liposome itself, and stabilization of its association with the modified chitosan. Cross-linking of lipids has been shown to improve liposome stability under the stress of surfactant addition.[22] In the present study, this would enhance the number of liposomes in the pellet, and therefore the amount of chitosan quantified in the re-suspension versus supernatant. However, since there was no difference between liposomes cross-linked before chitosan addition and those remaining uncross-linked, this cannot be the full picture. The improved stability of the post-adsorption cross-linked liposomes must also be explained in terms of the adsorption stabilization. Unlike the case of pre-adsorption cross-linked liposomes, the post-adsorption sample allows for complete insertion of the hydrophobic anchor, thus providing better anchoring in serum. Additionally, compared to liposomes that were not cross-linked, the reduced fluidity of the lipid bilayer reduces the likelihood of the anchor becoming detached from the outer leaflet. In this way, we hypothesize that the stability enhancement afforded by cross-linking after adsorption is a result of the ability of the18-carbon chain to insert into the bilayer, and remain inserted in the presence of elevated temperature and serum.

In consideration of differences in initial binding stoichiometry in conjunction with the percent desorbed, the molar amount of chitosan adsorbed per liposome after an hour in serum further demonstrates the utility of the post-adsorption cross-linked liposome (Figure 5b). Unlike Figure 3, glucosamine binding is stated per total lipid rather than

exposed lipid since some liposomes were likely ruptured during the incubation period. Uncross-linked liposomes had the same amount of DTPA-chitosan-g-C_{18} adsorbed as liposomes cross-linked post-adsorption initially. However, due to differences in stability, the amount remaining after an hour was almost half. Moreover, in comparing liposomes cross-linked before or after adsorption, the post-adsorption case represent a four-fold increase in the amount of chitosan adsorbed after an hour due to differences in initial stoichiometry as well as stability.

3.4 Magnetic Resonance Contrast Enhancement by Coated Liposomes

As pre- and post-adsorption cross-linked liposomes represented extremes in stabilization of the chitosan anchor, it was important to evaluate the functionality of the two systems in providing diagnostic capability. Gadolinium, which is chelated by DTPA, is used clinically to provide positive contrast in magnetic resonance images by coordinating with surrounding water molecules and shorting T_1 relaxation times. Gadolinium is always administered in the form of a chelate to mitigate concerns of toxicity. To load gadolinium on the liposome surface, cross-linked liposomes coated with DTPA-chitosan-g-C_{18} were titrated with gadolinium until all DTPA binding sites were saturated. This was verified by colorimetric titration with xylenol orange. This indicator solution is yellow in color, until coordinated with gadolinium, at which point the solution turns pink. DTPA has a much high binding affinity for gadolinium than xylenol orange, thus, xylenol orange can be used as an indicator to determine the presence of free, rather than chelated, gadolinium.[23] In the case of the coated liposomes, gadolinium was added

incrementally to an aliquot of liposome suspension in the presence of xylenol orange until the color change was observed.

After loading of the coated liposomes with gadolinium, samples were incubated for one hour in PBS supplemented with 10% human serum at 37 °C as in the adsorption stability study. Desorbed chitosan, loaded with gadolinium, was removed by centrifugation, and the remaining coated liposomes were used to create a concentration series of MR phantoms. Phantoms were placed in agar gels for imaging, and coronal cross sections were visualized with a 3 T clinical scanner using an IR-TSE sequence (Figure 6a).

As shown in Figure 6b, for any given lipid concentration, the signal intensity was much greater in the case of liposomes cross-linked after DTPA-chitosan-g-C_{18} adsorption. This is likely due to the higher concentration of gadolinium per liposome sample as a result of the differences in binding stoichiometry and desorption as discussed in Figure 5b. Gadolinium concentration was analyzed by ICP-OES to determine the differences in content. The amount of gadolinium present per lipid was nearly four-fold greater in the case of post-adsorption cross-linked liposomes, consistent with the observation that four times as much modified chitosan remained with post-adsorption cross-linked liposomes. To verify that differences in signal were due solely to differences in gadolinium concentration, it was necessary to calculate the molar relaxivity for the two cases.

For an IR-TSE sequence, the MR signal for a given inversion time, *TI*, is described by Equation 8:[24]

$$S(TI) = S_0\left[1-\left(1-k\right)e^{-TI/T_1}\right] \tag{8}$$

where S_0 represents signal at thermal equilibrium, k depends on flip angle and magnetization of the system, and T_1 is the spin-lattice relaxation time. As such, regions with shorter T_1 have brighter signal intensities. For example, fatty tissue has short T_1 and can often be distinguished from surrounding tissue in an MR image. The shortening of T_1 by gadolinium enhances signal in this way. The quantity 1/ T_1 is referred to as the relaxation rate, R_1 and is defined as follows:

$$R_1 = R_{1,water} + r_1[Gd] \tag{9}$$

where $R_{1,water}$ is the relaxation rate of contrast agent-free water, $[Gd]$ is the concentration of gadolinium, and r_1 is the molar relaxivity of the contrast agent. In this way, signal can be enhanced by higher gadolinium concentration or higher relaxivity.

For each phantom, T_1 was determined by three parameter nonlinear least squares fitting to Equation 8 as *TI* was varied. An example plot is shown in Figure 6c. Note from the shape of the curve that when signal would theoretically become negative, it is transposed across the *x*-axis to give positive signal in the resultant MR image. For the two cases, R_1 was plotted versus gadolinium concentration of each phantom to yield the relaxivity by linear regression of Equation 9. The relaxivity of pre-adsorption cross-linked liposomes was 6.52 ± 0.47 $mM^{-1}s^{-1}$, and that of post-adsorption liposomes was 6.50 ± 0.16 $mM^{-1}s^{-1}$. Since these values were equivalent, differences in signal intensity arose solely from differences in gadolinium concentration. The high loading of gadolinium per liposome makes the post-adsorption cross-linked liposomes superior for biomedical imaging, and in particular, targeted imaging. With the four-fold increase in loading, only one quarter of the amount of liposomes would be required to accumulate at a target site, compared to pre-adsorption cross-linked liposomes, to provide a given T_1

relaxation rate. Alternatively, the signal at the target would be greatly enhanced for any specific quantity of accumulated liposome.

Taken together, the results of these studies demonstrate the superior ability of liposomes cross-linked post chitosan adsorption to stably retain the chitosan anchor. In this way, these liposomes provided high MR contrast even after incubation in serum-supplemented media. To improve the chitosan anchor, the degree of substitution of DTPA could be increased to further augment the loading of gadolinium per liposome. Additionally, the number of alkyl chains per molecule could be increased to provide further binding stability. Such strategies for stabilization of micro- or nanoparticles will be critical for the development of future diagnostics or treatments that must remain stable until reaching their target site after injection. In this way, the system described in this study will be useful for a broad range of applications extending beyond surface loading of gadolinium.

3.5 Figures and Tables

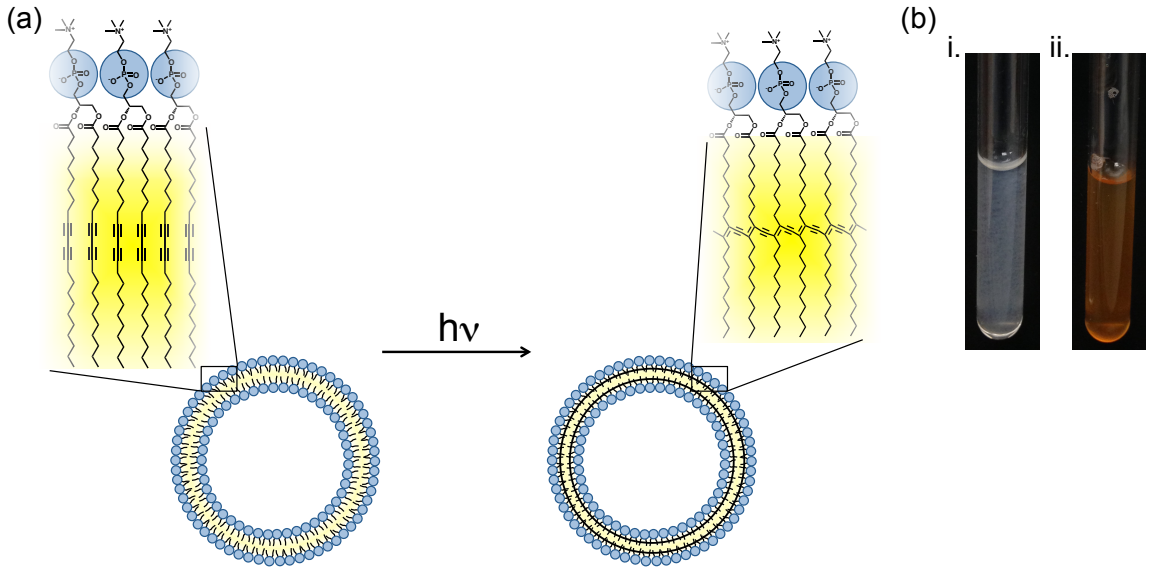

Figure 1. Liposomes with a continuous shell via cross-linking of bilayer. (a) Schematic depicting the photo-initiated polymerization of the lipid bilayer. (b) Liposome suspensions appear white in color prior to cross-linking (i), but turn orange after exposure to light at 254 nm (ii).

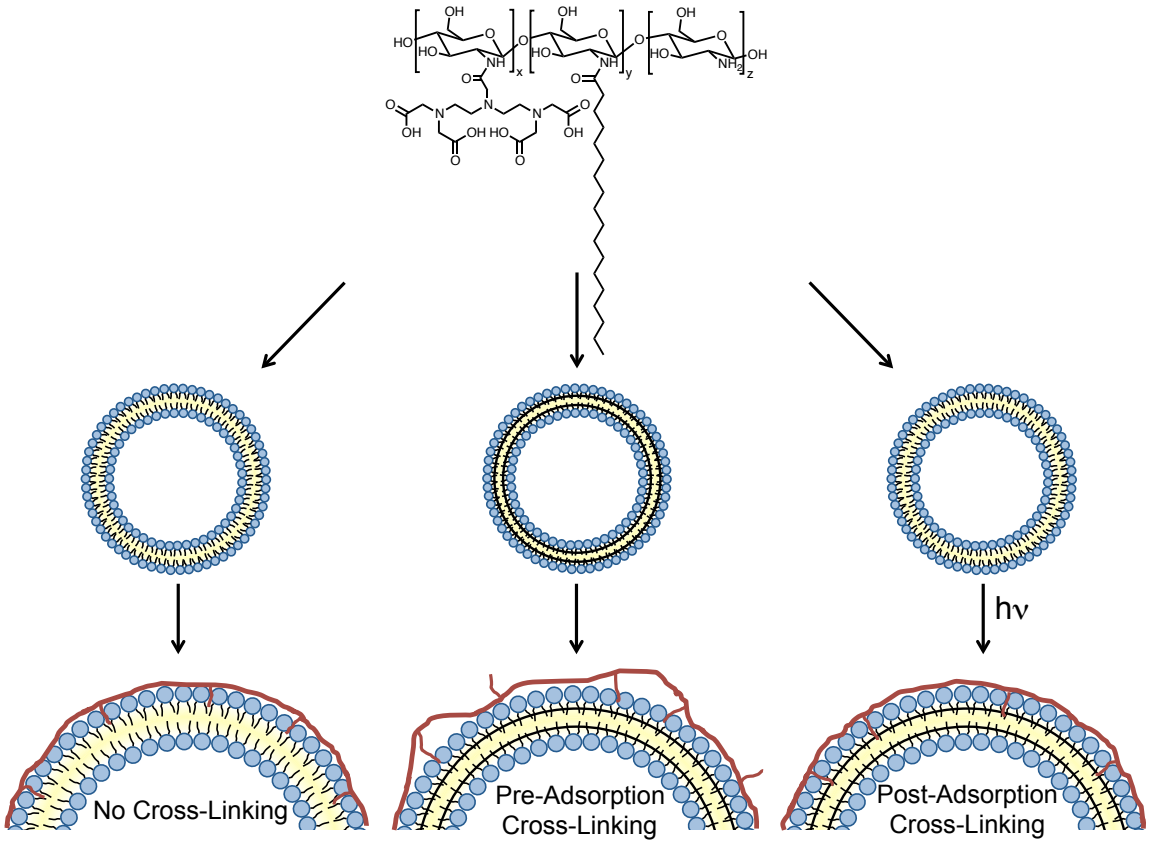

Figure 2. Schematic of association between DTPA-chitosan-g-C_{18} and $DC_{8,9}PC$ liposomes in three scenarios: (1) liposomes without a cross-linked bilayer, (2) liposomes cross-linked before association with chitosan, and (3) liposomes cross-linked after chitosan anchoring.

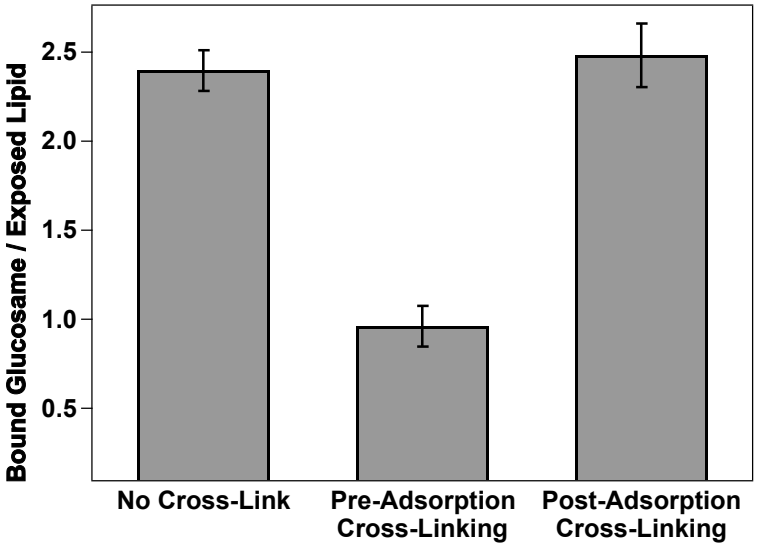

Figure 3. The number of glucosamine units bound per exposed lipid after adsorption to pre-formed liposomes in three different formulation conditions. Error bars represent standard deviation of four replicates per condition.

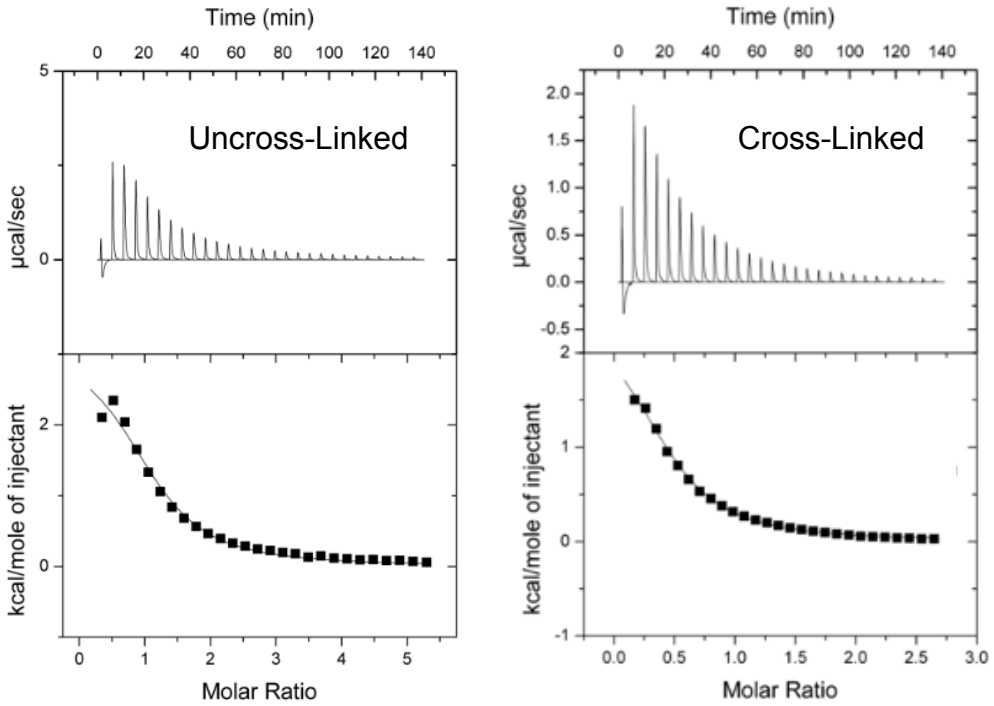

Figure 4. ITC thermograms comparing the heats of association between DTPA-chitosan-g-C_{18} and liposomes with uncross-linked bilayer or cross-linked bilayer. Heat flow data is shown in the top figure while the bottom figure represents fitting to a single-site binding model.

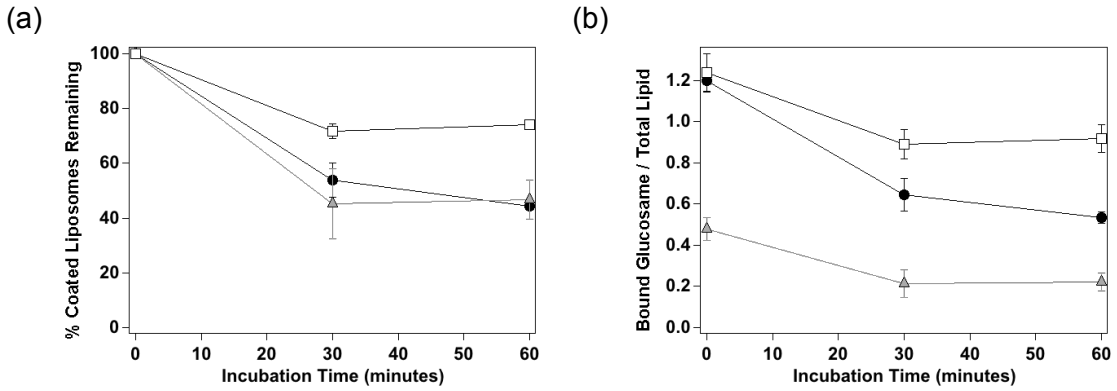

Figure 5. Stability of DTPA-chitosan-g-C_{18} in serum-supplemented media for the case of liposomes without cross-linked bilayer (●), pre-adsorption cross-linking of lipid bilayer (▲), and post-adsorption cross-linking of bilayer (□). (a) The percent remaining of the initial amount adsorbed. (b) The total amount of DTPA-chitosan-g-C_{18} remaining, per lipid dose. Error bars represent standard deviation of three replicates.

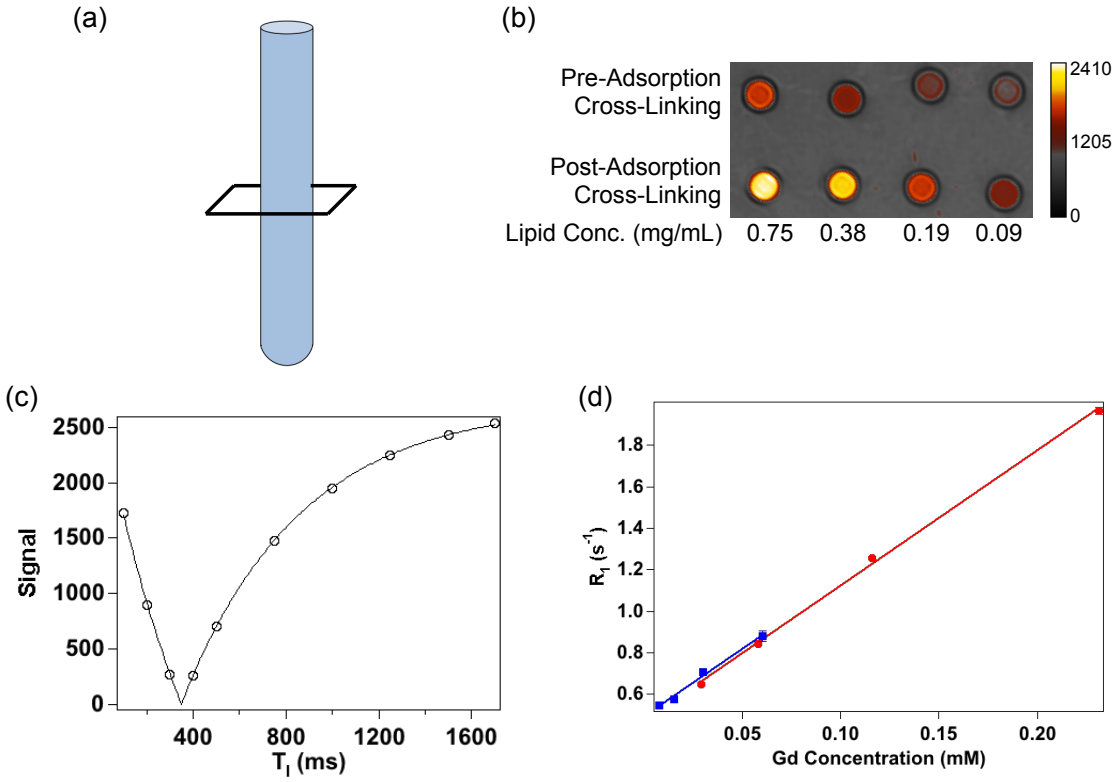

Figure 6. MR analysis of coated liposome phantoms. (a) Schematic of phantom solution with coronal cross section. (b) Pseudo-colored MR image of liposomes cross-linked before or after DTPA-chitosan-g-C_{18} adsorption (*TI* = 1250 ms). The concentration series is shown per lipid dose, and coloration represents signal intensity values. (c) Example intensity plot for determination of T_1 by varying *TI*. The plot shown is for post-adsorption cross-linked liposomes at a 0.75 mg/mL lipid concentration. (d) Gadolinium-based molar relaxivity plots for the two liposome samples. Error bars represent standard deviation of the fit parameter, and are predominantly obscured by data points.

Table 1. Binding parameters for the association between $DC_{8,9}PC$ liposomes and DTPA-chitosan-g-C_{18}. Molar amounts are listed per mole of glucosamine unit.

Liposome	N	K	ΔH	ΔG	ΔS
		10^4 M^{-1}	kcal/mol	kcal/mol	cal/mol•K
Uncross-Linked	1.10 ± 0.06	2.04 ± 0.33	3.14 ± 0.02	-5.87	30.2
Cross-Linked	0.46 ± 0.01	1.34 ± 0.08	2.50 ± 0.01	-5.62	27.3

Chapter 4

CONCLUSION

4.1 Summary

This study has demonstrated a strategy to stabilize liposomes coated with a functional anchor post-fabrication. The system consisted of liposomes made from cross-linkable $DC_{8,9}PC$ lipids, and chitosan modified with a hydrophobic anchor and the gadolinium chelate, DTPA. Three liposome systems were compared: liposomes that were never cross-linked, those that were cross-linked prior to addition of the functional chitosan, and those cross-linked after chitosan adsorption. While cross-linked liposomes are known to stabilize the system, the order of cross-linking versus adsorption was critical in formulation design. Liposomes that were cross-linked after chitosan was adsorbed were able to associate with a significantly greater number of glucosamine units of chitosan, and the chitosan that was adsorbed was far more stable in the presence of serum. This is likely due in part to the enhanced ability of the hydrophobic anchor to insert into the lipid bilayer and provide thermodynamically favorable binding, as supported by ITC, and remain inserted due to reduced mobility of lipids upon cross-linking. As a result, the MR signal enhancement per dose of liposome was dramatically increased compared to liposomes adsorbed with chitosan after cross-linking. Overall, this strategy of stabilizing a functional anchor to liposome surfaces extends beyond the system described. The same concept can be readily applied to anchors that impart enhanced targeting, multimodal imaging, or stealth capabilities, all of which would

benefit from surface localization and stability enhancement in the harsh environment of *in vivo* circulation.

4.2 Future Work

For future studies, it will be important to verify stability of the liposome itself in the presence of serum. Liposomes under stressed conditions release their encapsulated contents either by degradation and disassembly of the lipid bilayer, or by increased permeability of the vesicle that allows for release through a leaky bilayer. To test the former scenario, stability of liposomes is often measured by dynamic light scattering to record particle count or diameter of the sample over time.[22] For the latter case, stability can be monitored by leakage of a reporter molecule. For example, bovine serum albumin is often used as a model protein[25] in which slower release rates indicate greater liposome stability. Alternatively, fluorescent molecules are frequently exploited for their ability to quench within the liposome, and fluoresce when released. Calcein, a hydrophilic marker, can be encapsulated within the aqueous interior of the liposome,[26] while octadecylrhodamine B partitions in the hydrophobic bilayer.[27] In either case, liposome stability is monitored by measuring the increase in fluorescent intensity as the marker is released upon liposomal leaking or degradation.

We hypothesize that cross-linking the $DC_{8,9}PC$ liposomes will enhance their stability. The covalent polymerization creates a shell to limit degradation of the vesicle, and it has been shown previously by others that cross-linking of lipids enhances stability in the presence of the nonionic surfactant, Triton X-100.[22] In our case, we propose that the liposome system in which DTPA-chitosan-g-C_{18} is adsorbed prior to cross-linking

will be able to take advantage not only of the enhanced stability of the chitosan anchor, but will also have superior retention of encapsulated material compared to uncross-linked liposomes. This will be an area of interest in future studies.

REFERENCES

1. Rangel-Yagui, C. O.; Pessoa, A., Jr.; Tavares, L. C. Micellar Solubilization of Drugs. *J Pharm Pharm Sci* **2005,** *8*, 147-65.

2. Tan, J.; Shah, S.; Thomas, A.; Ou-Yang, H. D.; Liu, Y. The Influence of Size, Shape and Vessel Geometry on Nanoparticle Distribution. *Microfluid. Nanofluid.* **2013,** *14*, 77-87.

3. Xiao, K.; Li, Y.; Luo, J.; Lee, J. S.; Xiao, W.; Gonik, A. M.; Agarwal, R. G.; Lam, K. S. The Effect of Surface Charge on in Vivo Biodistribution of PEG-Oligocholic Acid Based Micellar Nanoparticles. *Biomaterials* **2011,** *32*, 3435-3446.

4. Gratton, S. E. A.; Ropp, P. A.; Pohlhaus, P. D.; Luft, J. C.; Madden, V. J.; Napier, M. E.; DeSimone, J. M. The Effect of Particle Design on Cellular Internalization Pathways. *Proc. Natl. Acad. Sci.* **2008,** *105*, 11613-11618.

5. Ayyagari, A. L.; Zhang, X.; Ghaghada, K. B.; Annapragada, A.; Hu, X.; Bellamkonda, R. V. Long-Circulating Liposomal Contrast Agents for Magnetic Resonance Imaging. *Magn. Reson. Med.* **2006,** *55*, 1023-1029.

6. Byrne, J. D.; Betancourt, T.; Brannon-Peppas, L. Active Targeting Schemes for Nanoparticle Systems in Cancer Therapeutics. *Adv. Drug Del. Rev.* **2008,** *60*, 1615-1626.

7. Peters, D.; Kastantin, M.; Kotamraju, V. R.; Karmali, P. P.; Gujraty, K.; Tirrell, M.; Ruoslahti, E. Targeting Atherosclerosis by Using Modular, Multifunctional Micelles. *Proc. Natl. Acad. Sci.* **2009**.

8. Tian, M.; Qin, A.; Ramireddy, C.; Webber, S. E.; Munk, P.; Tuzar, Z.; Prochazka, K. Hybridization of Block Copolymer Micelles. *Langmuir* **1993,** *9*, 1741-1748.

9. Owens III, D. E.; Peppas, N. A. Opsonization, Biodistribution, and Pharmacokinetics of Polymeric Nanoparticles. *Int. J. Pharm.* **2006,** *307*, 93-102.

10. Moghimi, S. M.; Szebeni, J. Stealth Liposomes and Long Circulating Nanoparticles: Critical Issues in Pharmacokinetics, Opsonization and Protein-Binding Properties. *Prog. Lipid Res.* **2003,** *42*, 463-478.

11. Lu, J.; Owen, S. C.; Shoichet, M. S. Stability of Self-Assembled Polymeric Micelles in Serum. *Macromolecules* **2011,** *44*, 6002-6008.

12. Taira, M. C.; Chiaramoni, N. S.; Pecuch, K. M.; Alonso-Romanowski, S. Stability of Liposomal Formulations in Physiological Conditions for Oral Drug Delivery. *Drug Deliv.* **2004,** *11*, 123-128.

13. Kamaly, N.; Xiao, Z.; Valencia, P. M.; Radovic-Moreno, A. F.; Farokhzad, O. C. Targeted Polymeric Therapeutic Nanoparticles: Design, Development and Clinical Translation. *Chem. Soc. Rev.* **2012,** *41*, 2971-3010.

14. Punnamaraju, S.; You, H.; Steckl, A. J. Triggered Release of Molecules across Droplet Interface Bilayer Lipid Membranes Using Photopolymerizable Lipids. *Langmuir* **2012,** *28*, 7657-7664.

15. Mertins, O.; Dimova, R. Binding of Chitosan to Phospholipid Vesicles Studied with Isothermal Titration Calorimetry. *Langmuir* **2011,** *27*, 5506-5515.

16. Quemeneur, F.; Rinaudo, M.; Maret, G.; Pepin-Donat, B. Decoration of Lipid Vesicles by Polyelectrolytes: Mechanism and Structure. *Soft Matter* **2010,** *6*, 4471-4481.

17. ITC Data Analysis in Origin. In *Tutorial Guide*, 5th ed.; MicroCal LLC: Northampton, MA, 1998.

18. Ho, J. K.; Duclos, R. I.; Hamilton, J. A. Interactions of Acyl Carnitines with Model Membranes: A ^{13}C-NMR Study. *J. Lipid Res.* **2002,** *43*, 1429-1439.

19. Meier, M.; Seelig, J. Lipid and Peptide Dynamics in Membranes Upon Insertion of N-Alkyl-Beta-D-Glucopyranosides. *Biophys. J.* **2010,** *98*, 1529-38.

20. Fennell, C.; Dill, K. Physical Modeling of Aqueous Solvation. *J Stat Phys* **2011,** *145*, 209-226.

21. Tanford, C., *The Hydrophobic Effect: Formation of Micelles and Biological Membranes*. Wiley and Sons: New York, 1973.

22. Liu, S.; O'Brien, D. F. Stable Polymeric Nanoballoons: Lyophilization and Rehydration of Cross-Linked Liposomes. *J. Am. Chem. Soc.* **2002,** *124*, 6037-6042.

23. Barge, A.; Cravotto, G.; Gianolio, E.; Fedeli, F. How to Determine Free Gd and Free Ligand in Solution of Gd Chelates. A Technical Note. *Contrast Media & Molecular Imaging* **2006,** *1*, 184-188.

24. Rohrer, M.; Bauer, H.; Mintorovitch, J.; Requardt, M.; Weinmann, H. J. Comparison of Magnetic Properties of MRI Contrast Media Solutions at Different Magnetic Field Strengths. *Invest. Radiol.* **2005,** *40*, 715-724.

25. Ntimenou, V.; Mourtas, S.; Christodoulakis, E. V.; Miltiadis, T.; Antimisiaris, S. G. Stability of Protein-Encapsulating DRV Liposomes after Freeze-Drying: A Study with BSA and t-PA. *J. Liposome Res.* **2006,** *16*, 403-416.

26. Kaviratna, A. S.; Banerjee, R. The Effect of Acids on Dipalmitoyl Phosphatidylcholine (DPPC) Monolayers and Liposomes. *Colloids Surf. Physicochem. Eng. Aspects* **2009,** *345*, 155-162.

27. Domecq, A.; Disalvo, E. A.; Bernik, D. L. A Stability Test of Liposome Preparations Using Steady-State Fluorescent Measurements. *Drug Deliv.* **2001,** *8*, 155-160.